Quaternary Science Reviews 107 (2015) 138–148

Contents lists available at ScienceDirect

Quaternary Science Reviews

journal homepage: www.elsevier.com/locate/quascirev

Influence of tropical easterlies in southern Africa's winter rainfall zone during the Holocene

Brian M. Chase [a, b, *], Sophak Lim [a], Manuel Chevalier [a], Arnoud Boom [c], Andrew S. Carr [c], Michael E. Meadows [d], Paula J. Reimer [e]

[a] Centre National de Recherche Scientifique, UMR 5554, Institut des Sciences de l'Evolution de Montpellier, Université Montpellier 2, Bat.22, CC061, Place Eugène Bataillon, 34095, Montpellier Cedex 5, France
[b] Department of Archaeology, History, Culture and Religion, University of Bergen, Postbox 7805, 5020, Bergen, Norway
[c] Department of Geography, University of Leicester, Leicester, LE1 7RH, UK
[d] Department of Environmental and Geographical Science, University of Cape Town, Private Bag X3, Rondebosch, 7701, South Africa
[e] School of Geography, Archaeology and Palaeoecology, Queen's University Belfast, Belfast, BT7 1NN, Northern Ireland, UK

A R T I C L E I N F O

Article history:
Received 5 July 2014
Received in revised form
11 October 2014
Accepted 13 October 2014
Available online 10 November 2014

Keywords:
Quaternary
Holocene
Southern Africa
Rock hyrax midden
Palaeoclimate
$\delta^{13}C$
$\delta^{15}N$
Pollen
Climate change

A B S T R A C T

South Africa's southwestern Cape occupies a critical transition zone between Southern Hemisphere temperate (winter) and tropical (summer) moisture-bearing systems. In the recent geological past, it has been proposed that the relative influence of these systems may have changed substantially, but little reliable evidence regarding regional hydroclimates and rainfall seasonality exists to refine or substantiate the understanding of long-term dynamics. In this paper we present a mid-to late Holocene multi-proxy record of environmental change from a rock hyrax midden from Katbakkies Pass, located along the modern boundary between the winter and summer rainfall zones. Derived from stable carbon and nitrogen isotopes, fossil pollen and microcharcoal, these data provide a high resolution record of changes in humidity, and insight into changes in rainfall seasonality. Whereas previous work concluded that the site had generally experienced only subtle environmental change during the Holocene, our records indicate that significant, abrupt changes have occurred in the region over the last 7000 years. Contrary to expectations based on the site's location, these data indicate that the primary determinant of changes in humidity is summer rather than winter rainfall variability, and its influence on drought season intensity and/or length. These findings are consistent with independent records of upwelling along the southern and western coasts, which indicate that periods of increased humidity are related to increased tropical easterly flow. This substantially refines our understanding of the nature of temperate and tropical circulation system dynamics in SW Africa, and how changes in their relative dominance have impacted regional environments during the Holocene.

1. Introduction

Southwestern Africa lies at the boundary between Southern Hemisphere temperate and tropical climate systems (Tyson, 1986). Presently, much of the region's precipitation falls during the austral winter months, when expansions of the circumpolar vortex bring the westerly storm track and its associated frontal systems into closer contact with the subcontinent. Conversely, the region experiences a marked summer drought period, as (1) it lies distal to the primary tropical moisture source of the Indian Ocean, and (2) seasonal displacements the South Atlantic Anticyclone intensify upwelling along the west coast, blocking the westward propagation of easterly waves that bring summer rainfall to much of southern Africa. During the late Quaternary, the region is thought to be sensitive to long-term changes in these systems as a function of changes in global boundary conditions (see van Zinderen Bakker, 1976; Cockroft et al., 1988; Chase and Meadows, 2007). However, while the relative dominance of these climate systems may have changed significantly during the late Quaternary, the region's strongly seasonal climates generally preclude the preservation of organic material, and very little terrestrial evidence exists to refine our understanding of their past dynamics (e.g. Martin, 1968; Scholtz, 1986; Carr et al., 2006). Despite this constraint, records of environmental change can be obtained from archives that are not

* Corresponding author. Institut des Sciences de l'Evolution de Montpellier, UMR 5554, Centre National de Recherche Scientifique/Université Montpellier 2, Bat.22, CC061, Place Eugène Bataillon, 34095, Montpellier Cedex 5, France.
E-mail address: brian.chase@univ-montp2.fr (B.M. Chase).

http://dx.doi.org/10.1016/j.quascirev.2014.10.011

subject to deterioration by the region's climate. Notably, proxy records obtained from marine cores (Farmer et al., 2005; Weldeab et al., 2013) and stable isotope records from archaeological deposits (Cohen et al., 1992; Cohen and Tyson, 1995), although containing records of inherently contrasting temporal resolution, have provided some indications of changes in regional atmospheric circulation dynamics, particularly those manifested in variations in coastal upwelling regimes. Key among hypotheses derived from these data is the mechanistic model developed by Cohen and Tyson (1995), which posits that lower (higher) near-coastal SSTs along the south coast would be associated with increased (decreased) upwelling along the south coast, and increased tropical easterly (temperate westerly) flow. This variability was linked to overall wetter (drier) conditions in the continental interior, which is part of southern Africa's summer rainfall zone, and derives most its moisture from the tropical easterlies. Recent studies of rock hyrax middens from the southern Cape Fold Mountains (Chase et al., 2013) have lent some support this model, finding that regional trends in water availability during the Holocene correlate strongly with higher south coast SSTs, continental temperature records (Talma and Vogel, 1992 [chronology after Chase et al., 2013]), and remote evidence for shifts in the westerly storm track (Lamy et al., 2001), which in turn can be linked to changes in Antarctic sea-ice extent (Fischer et al., 2007; Wolff et al., 2010). These findings highlight the importance of temperate moisture-bearing systems in the southwestern and southern Cape, but lacking are records from the western interior that indicate the extent to which increases in easterly flow may have brought increased summer rainfall to regions distal to the primary Indian Ocean moisture source.

In this paper, we present fossil pollen, microcharcoal, and high resolution stable isotope ($\delta^{13}C$ and $\delta^{15}N$) records from a rock hyrax (*Procavia capensis*) midden from Katbakkies Pass in South Africa's Swartruggens Mountains, strategically located on the modern winter–summer rainfall zone boundary. These data provide detailed information regarding both past vegetation and hydroclimatic change, providing a first opportunity to assess the relative roles of temperate westerly and tropical easterly systems in driving climate change in southwestern Africa during the Holocene.

1.1. Regional setting

The Swartruggens Mountains are a southeastern subsidiary range of the Cederberg Mountains, which dominate the north–south axis of the Cape Fold Mountains to the east and northeast of Cape Town (Fig. 1). Extending for ~300 km parallel to the Atlantic Ocean (50–100 km to the west), this portion of the Cape Fold Belt is, in its northern portion, a significant divide between the relatively humid climates of the southwestern Cape and the arid Karoo, which dominates much of South Africa's western continental interior. The range also broadly marks the divide between southern Africa's two major climate regimes: the winter rainfall zone to the west and the summer rainfall zone to the northeast (cf. Chase and Meadows, 2007). The winter rainfall zone is defined by the seasonal intensification and northward expansion of the westerlies and associated frontal depressions that transport moisture to the region during the austral winter months. To the east, and across most of South Africa, tropical easterly flow transports moisture from the Indian Ocean during the austral summer (Fig. 1; Tyson, 1986; Tyson and Preston-Whyte, 2000). The Cederberg and adjacent ranges act as an orographic divide between these climate zones, with the mountains creating a distinct rainshadow for westerly derived rainfall. The higher elevations receive five times the precipitation of the lowlands to the east, but more importantly, while the mountains receive more than 75% of their rainfall during the winter, the

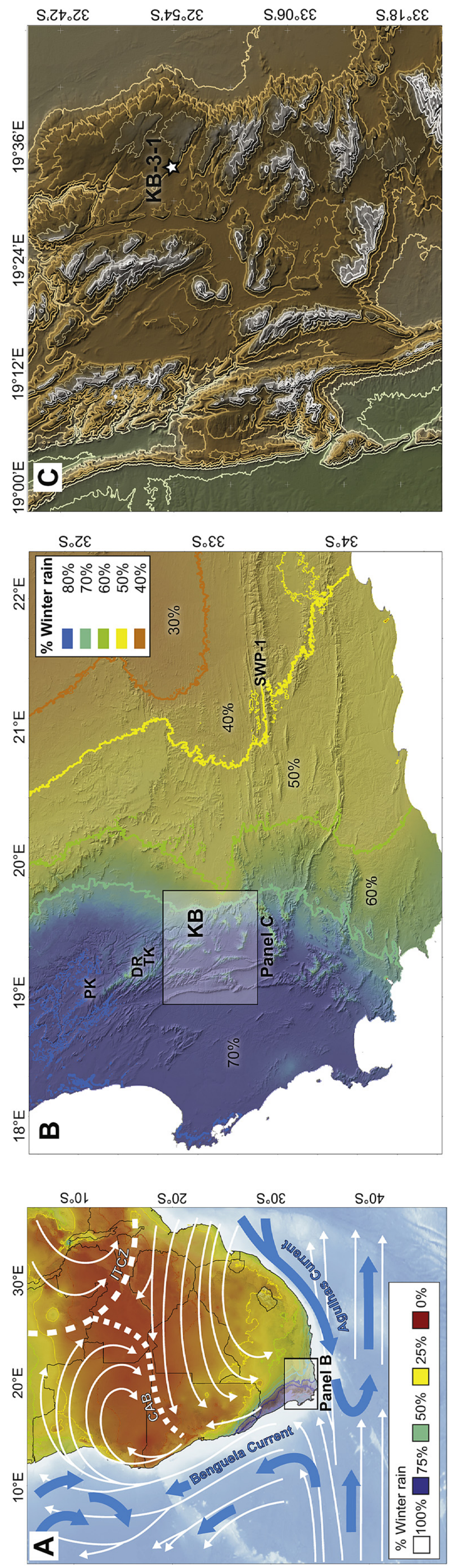

Fig. 1. (A) Map of southern Africa showing seasonality of rainfall and sharp climatic gradients dictated by the zones of summer/tropical (red) and winter/temperate (blue) rainfall dominance. Winter rainfall is primarily a result of storm systems embedded in the westerlies. Major atmospheric (white arrows) and oceanic (blue arrows) circulation systems and the austral summer positions of the Inter-Tropical Convergence Zone (ITCZ) and the Congo Air Boundary (CAB) are indicated. The location of the study site in the southwestern Cape region is shown. (B) Map of southwestern Cape with the Katbakkies Pass site and other hyrax midden sites indicated (PK, Pakhuis Pass (Scott and Woodborne, 2007a, b); DR, De Rif (Chase et al., 2011; Quick et al., 2011; Valsecchi et al., 2013); TK, Truitjes Kraal (Meadows et al., 2010); SWP-1; Seweweekspoort-1 (Chase et al., 2013)). (C) Topographical map of Katbakkies Pass (200 m contours), with the KB-3-1 site indicated. (For interpretation of the references to colour in this figure legend, the reader is referred to the web version of this article.)

lowlands to the east currently receives 50% or more of their precipitation during the summer (Hijmans et al., 2005).

Katbakkies Pass is located on the eastern slopes of the Cape Fold Mountains, and is thus optimally placed to record changes in the effectiveness and influence of easterly versus westerly moisture bearing systems (Fig. 1). Mean annual rainfall at the site is ~300 mm/yr, ~70% of which falls in the austral winter months between April and September (Hijmans et al., 2005). While wetlands can be found at higher elevations (e.g. the Driehoek Valley; Meadows and Sugden, 1991, 1993), they are rare, and few palaeoenvironmental records have been obtained from the region. Recent work, however, has demonstrated the potential of rock hyrax middens – accumulations of dried urine and faecal pellets – as archives for a range of palaeoenvironmental proxies (Chase et al., 2012). For this study, a midden (KB-3-1; 32.896°S, 19.561°E; 1170 m amsl.) was collected from a northwest-facing cliff, approximately 100 m up valley from the midden complex described by Meadows et al. (2010).

The vegetation at the site is classified as Swartruggens Quartzite Fynbos, a more arid form of fynbos, defined by asteraceous and proteoid elements (Mucina and Rutherford, 2006). In the open landscape around the site, species of Asteraceae (esp. *Elytroppapus* sp., *Euryops* sp., *Eriocephalus* sp., *Stoebe* sp.) are particularly common, as are Restionaceae and succulent species of Aizoaceae and Crassulaceae. The site itself is found in a narrow gorge, and the favourable hydrology and protection from fire promotes the growth of Cape thicket elements including *Maytenus oleoides*, *Dodonaea viscosa*, *Protea* sp., *Leucadendron* sp. and *Rhus* sp.. Below the pass, 2 km to the southeast, is the Riet River, the riparian zone and flood plain of which is densely vegetated with species of Cyperaceae, Restionaceae and Poaceae.

2. Material and methods

Similar to midden sections previously collected from Katbakkies Pass (Meadows et al., 2010), selection of the material was based on its high hyraceum (crystallised urine) relative to faecal pellet content. Apart from having greater structural integrity and less variable deposition rates, hyraceum is thought to represent environmental conditions more clearly than samples containing faecal pellets, which may potentially include a degree of dietary bias (Chase et al., 2012). A representative portion was removed from the larger KB-3-1 midden complex, and cut perpendicular to the stratigraphy using an angle grinder. The nature of the shelter in which the midden developed had resulted in stepped morphology of the deposit, and for sampling two overlapping sections (upper and lower sections being 120 mm and 285 mm in depth respectively) were cut and subsequently polished for subsampling. The sections are separated at 3335 cal BP.

2.1. Chronology

Radiocarbon age determinations were processed at the ^{14}CHRONO Centre, Queen's University Belfast using accelerator mass spectrometry (AMS). The radiocarbon ages were calibrated using CALIB 7.0 with the SHCal13 calibration data (Hogg et al., 2013) (Table 1), and the Bacon 2.2 software package (Blaauw and Christen, 2011) was used to generate the age–depth models (Fig. 2).

2.2. Stable isotopes

Stable isotope analysis of bulk midden samples were performed at the Department of Archaeology, University of Cape Town according to the methods described in Chase et al. (2010, 2009), with contiguous/overlapping samples obtained from two series of offset 1 mm holes. The standard deviation derived from replicate analyses of homogeneous material was better than 0.2‰ for both carbon and nitrogen. Carbon isotope results are expressed relative to Vienna PDB. Nitrogen isotope results are expressed relative to atmospheric nitrogen.

2.3. Pollen and microcharcoal

For fossil pollen and microcharcoal analysis, contiguous blocks of material 2–5 mm thick and weighing between ~0.3 g and 1.0 g were cut from the section parallel to the radiocarbon and stable isotope samples. Pollen samples were prepared with standard physical (600 μm sieving and decanting) and chemical (HCl, KOH, HF and acetolysis) methods (Moore et al., 1991). *Lycopodium* tablets were added to the weighed sample to estimate pollen concentrations (Stockmarr, 1971). A minimum pollen sum of 400 grains was counted at a magnification of ×400 under a light microscope, and

Table 1
Radiocarbon ages and calibration information for the upper and lower sections of the KB-3-1 hyrax midden.

Sample	Depth (mm)	^{14}C age BP	1 sigma Error	Calibration data	95.4% (2σ) cal age ranges	Relative area under distribution	Median probability
Upper section							
UBA-20657	11.7	1008	44	SHCal13	cal BP 774–938	0.98	860
					cal BP 944–954	0.02	
UBA-21362	84.9	2585	48	SHCal13	cal BP 2440–2448	0.005	2613
					cal BP 2457–2759	0.995	
UBA-20658	169.6	3791	56	SHCal13	cal BP 3914–4295	0.997	4110
					cal BP 4335–4338	0.002	
					cal BP 4343–4345	0.002	
Lower section							
UBA-21363	2.1	3085	54	SHCal13	cal BP 3073–3377	1	3243
UBA-20660	93.6	3869	74	SHCal13	cal BP 3986–4050	0.065	4231
					cal BP 4062–4423	0.935	
UBA-20661	160.1	4065	54	SHCal13	cal BP 4298–4328	0.019	4503
					cal BP 4352–4370	0.012	
					cal BP 4384–4651	0.877	
					cal BP 4670–4702	0.025	
					cal BP 44758–4808	0.068	
UBA-21364	221.9	4717	68	SHCal13	cal BP 5086–5100	0.007	5412
					cal BP 5141–5159	0.01	
					cal BP 5284–5588	0.982	
UBA-20662	293.4	6204	72	SHCal13	cal BP 6860–6871	0.007	7060
					cal BP 6880–7254	0.993	

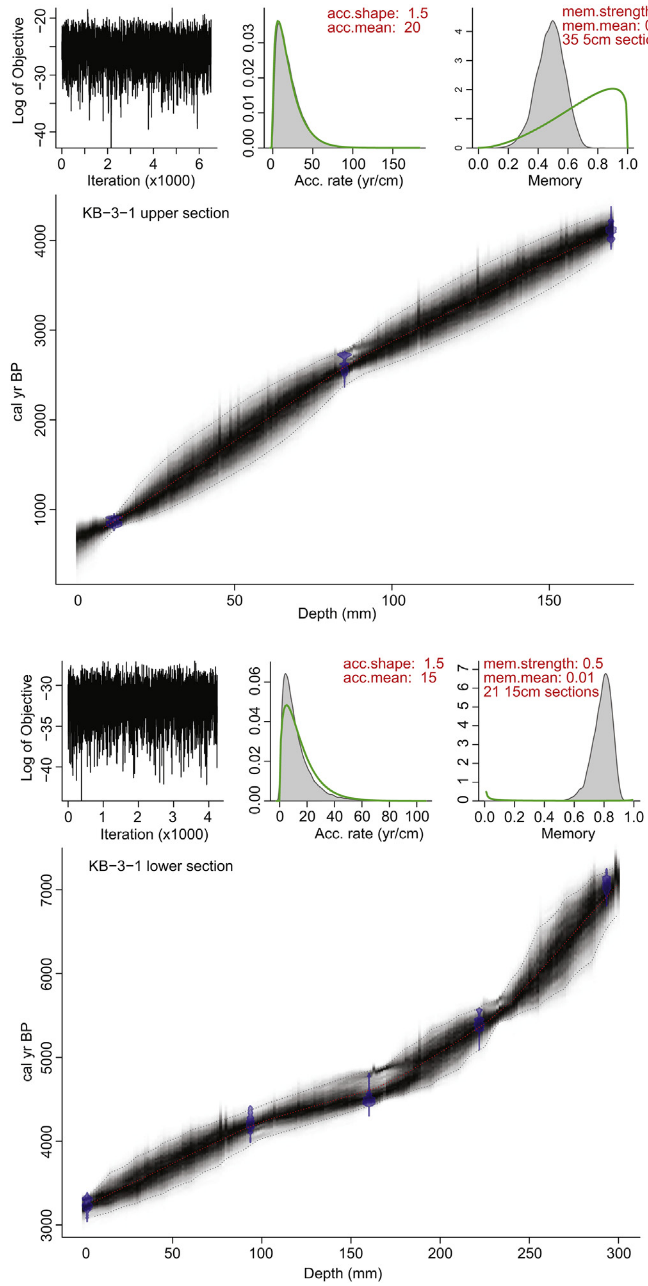

Fig. 2. Age models for the KB-3-1 hyrax midden.

identified with the help of the literature (Scott, 1982; van Zinderen Bakker, 1953, 1956; van Zinderen Bakker and Coetzee, 1959), and photographic and slides reference collections at the University of the Free State, University of Cape Town, and University of Montpellier. Microcharcoal particles were identified as black, completely opaque, angular fragments that occurred in the pollen slides (Clark, 1988). Only charcoal particles >75 μm^2 (or longer than 10 μm) were counted under a light microscope at ×400 magnification. A minimum count of 200 items (given by the sum of charcoal particles and exotic marker grains) was used. Charcoal particles which exceed the mesh-width size of 600 μm are missing from the microscopic charcoal record and particles of ca <10 μm were not counted in order to ensure correct identification. The charcoal signal is thus generally related primarily to the regional fire signal, with local fires (large particles) not being differentiated, and extra-regional fires (<10 μm particles) being excluded. Previous calibration studies indicate that the regional origin of microscopic charcoal of the identified size range is likely to be between 2 and 50 km from the site (Tinner et al., 1998; Conedera et al., 2009).

The TILIA program (Grimm, 2011) was used to construct the pollen diagrams and to detect changes in pollen composition and define pollen zones using constrained hierarchical clustering by sum of squares. For a full description of hyrax middens, their development and the sampling and analytical methodologies for the proxies they contain, see Chase et al. (2012).

2.4. Climate reconstruction from pollen data

To identify and quantify variations in winter and summer rainfall from the Katbakkies pollen data we used the climate reconstruction method designed by Chevalier et al. (2014), and the associated software package CREST. This method statistically estimates the link between plants and climate using probability density functions (*pdfs*). When applied to pollen data, the estimate of a given pollen type's *pdf* for a specific climate parameter follows two steps: 1) a parametric *pdf* is fitted to all the species belonging to the pollen type, and 2) the species *pdfs* are combined into a pollen type *pdf*. To reconstruct cold and warm quarter precipitation, lognormal *pdfs* were fitted for the species. For more details on the method and software, see Chevalier et al. (2014)

For this study, climate data are derived from the WorldClim1.4 dataset (Hijmans et al., 2005), and botanical data were extracted from a series of databases held by the South African National Biodiversity Institute (http://sibis.sanbi.org/faces/DataSources.jsp; Rutherford et al., 2012, 2003; SANBI, 2003). The botanical data, which are derived mainly from herbarium collections and documented observations, are available as ‘presence’, generally within a particular 0.25° × 0.25°grid square. We have used this resolution for our analyses, upscaling more precisely georeferenced data to this common resolution. For each pollen type we have excluded all species whose presence was not recorded within a 300 km radius around the site.

Not all the pollen types identified in the different samples were used to reconstruct the two precipitation variables presented here. Pollen types composed of hundreds of undifferentiated plant species occupying diverse habitats (e.g. Asteraceae, Poaceae, Restionaceae, Scrophulariaceae) are climatically non-informative (i.e. at this taxonomic resolution, the species comprising the pollen type occupy excessively diverse climate ranges), and were excluded. In the context of the site, pollen types observed in our analysis to be insensitive to the winter and summer rainfall amount – such as the temperature sensitive pollen types *Anthospermum*-type, Ericaceae and *Stoebe*-type – were also excluded. For some pollen types, too few records ($n < 25$) were available for robust *pdfs* to be calculated (e.g. *Myrica* and *Myrothamnus*). The initial set of 45 pollen-types was thus reduced to 27 precipitation-sensitive pollen types. To remove noise from the reconstructions, pollen percentages lower than 0.2% were set to 0.

3. Results

3.1. Chronology

Radiocarbon analyses indicate that the KB-3-1 midden accumulated during the mid-to late Holocene, between ~700 and 7000 cal (calibrated) BP. The age–depth models for the two overlapping sections suggest continuous deposition, with no obvious hiatuses (Table 1; Fig. 2). Accumulation rates for KB-3-1 average ~56 $\mu m\ yr^{-1}$, with lower rates (~40 $\mu m\ yr^{-1}$) in the upper and lower portions of the record, and increasing rates (as high as

~248 μm yr^{-1}) during the mid-Holocene, ca 4500 cal BP. Each 1 mm isotope sample therefore integrates between approximately ~4–24 years of hyraceum accumulation. A horizontal fracture in the midden resulted in a break in the record from ~4250 to 4590 cal BP.

As was observed at KB-1 (Meadows et al., 2010), KB-3-1 ceased accumulating several hundred years ago. This is not an uncommon phenomenon at midden sites, with accumulation stopping when the middens fill the shelter to the extent that the animals can no longer enter (Chase et al., 2012). This was clearly the case with the KB-3-1 midden, and the cessation of accumulation is not an indication of changes in environmental conditions.

3.2. Stable isotopes

The δ^{13}C and δ^{15}N values from the KB-3-1 midden vary from −24.6 to −26.5‰ and from 0.96 to 5.6‰ respectively (Fig. 3). At Katbakkies, which is within the Fynbos biome and dominated by vegetation using the C_3 photosynthetic pathway, midden δ^{13}C is interpreted to primarily reflect changes in plant water-use efficiency. Therein, more humid conditions are reflected in more depleted δ^{13}C values as determined by water availability and temperature (Ehleringer and Cooper, 1988; Pate, 2001; Chase et al., 2011). The absolute values and muted amplitude of the δ^{13}C record is consistent with changes in water-use efficiency being the primary determinant of δ^{13}C variability. The presence of succulent plant species may influence the record to some extent, and such plants have leaf δ^{13}C values between −24 and −14‰, tending to higher values for obligate CAM photosynthesis (Boom et al., 2014). The δ^{13}C values from the KB-3-1 midden do not, however, indicate significant CAM contributions, which would at any rate have a similar palaeoenvironmental interpretation as increasing water-use efficiency.

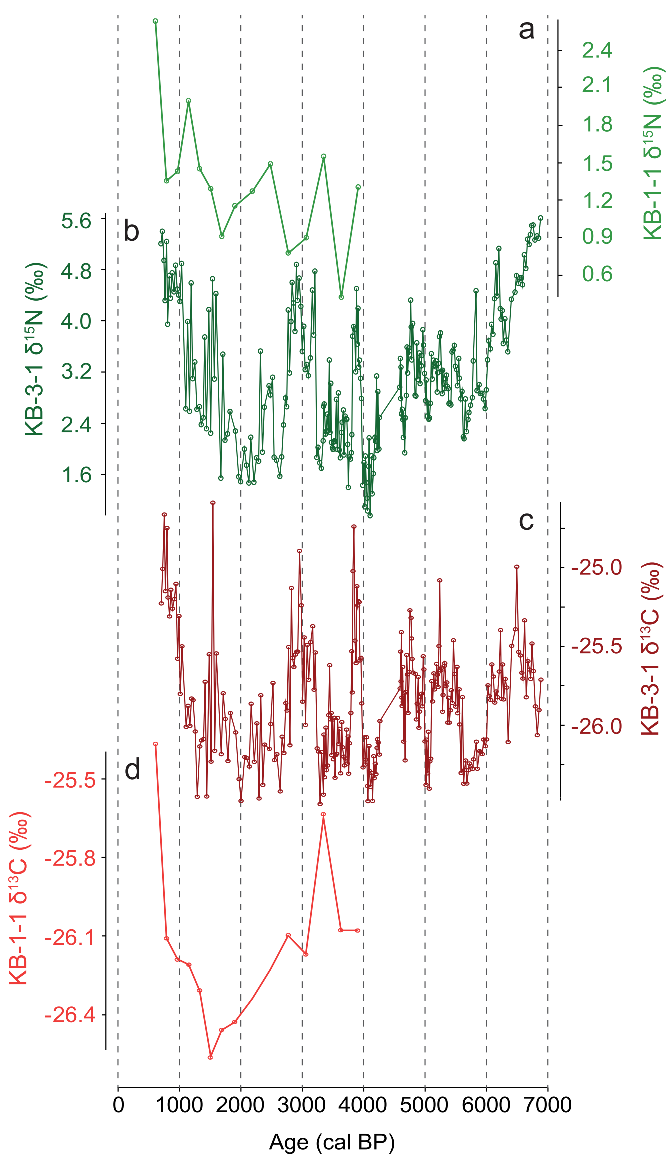

Fig. 3. δ^{15}N and δ^{13}C values from the KB-3-1 (b, c) and KB-1 (a, d; Meadows et al., 2010) hyrax midden.

As in other studies, changes in midden δ^{15}N are interpreted to reflect changes in water availability (see more extensive discussion in Chase et al., 2012). In brief, there are recognised links between aridity and foliar ^{15}N at the global scale (e.g. Craine et al., 2009; Hartman and Danin, 2010), the replication of this signal in animal and plant tissues (e.g. Murphy and Bowman, 2006; Hartman, 2011; Newsome et al., 2011). In our own studies we see consistently strong correlations between midden ^{15}N and several independent climatic proxy records, suggesting that environmental moisture availability (though not specifically mean annual precipitation) is a major driver of midden ^{15}N records (Chase et al., 2009, 2010, 2011). These patterns may be influenced to some extent by other (e.g. microclimatic) factors, and while being potentially complex – as is reflected in the variability observed in the relationship between modern foliar ^{15}N and aridity estimates (e.g. Murphy and Bowman, 2006; Hartman and Danin, 2010; Peri et al., 2012) – the strong negative correlation observed between the δ^{15}N and δ^{13}C records at Katbakkies ($r^2 = 0.78$, $p < 10^{-4}$) implies that both are responding to the same environmental forcing. The results presented here from the KB-3-1 midden are, considering differences in sampling resolution and age models, consistent with the results from the KB-1 midden reported by Meadows et al. (2010; Fig. 3).

Following the above, the isotope records indicate a marked increase in humidity from ~6900 to 5600 cal BP across the early to mid-Holocene transition. A period of relative environmental stability is observed from ~5600 to 4700 cal BP, followed by a relatively humid period from ~4700 to 3200 cal BP. This phase is punctuated by a distinct arid event at 4000–3800 cal BP, and terminates with a longer arid episode from 3200 to 2700 cal BP. This followed by a period of increased water-availability comparable to the 4700–3200 period, which last from 2700 cal BP to approximately 1700 cal BP, when a series of high frequency, high amplitude changes mark the beginning of a trend toward drier conditions at the end of the record.

3.3. Fossil pollen and microcharcoal

Similar to the findings of Meadows et al. (2010), relatively little change is observed in the pollen records from the KB-3-1 midden (Fig. 4). Despite the diversity of pollen types identified, which represent fynbos thicket (Celastraceae, Myricaceae, Myrtaceae, *Dodonaea*, *Phylica*, *Podocarpus* and *Rhus*-type), fynbos (Ericaeae, *Blaeria*, Proteaceae, Restionaceae, *Cliffortia*), and a variety of succulent (Aizoaceae, Crassulaceae, Euphorbiacae, *Aloe*-type) and asteraceous taxa (Asteraceae, *Pentzia*-type, *Stoebe*-type, *Berkheya*-type, *Felicia*), little, if any, replacement of taxa is observed, and percentage variations within each pollen type are muted. Moreover, the best represented pollen types (Asteraceae, Restionaceae and Cyperaceae) are, at Katbakkies, ambiguous in terms of their palaeoenvironmental significance.

Four pollen zones were determined by constrained hierarchical clustering, and some changes in the pollen assemblage consistent

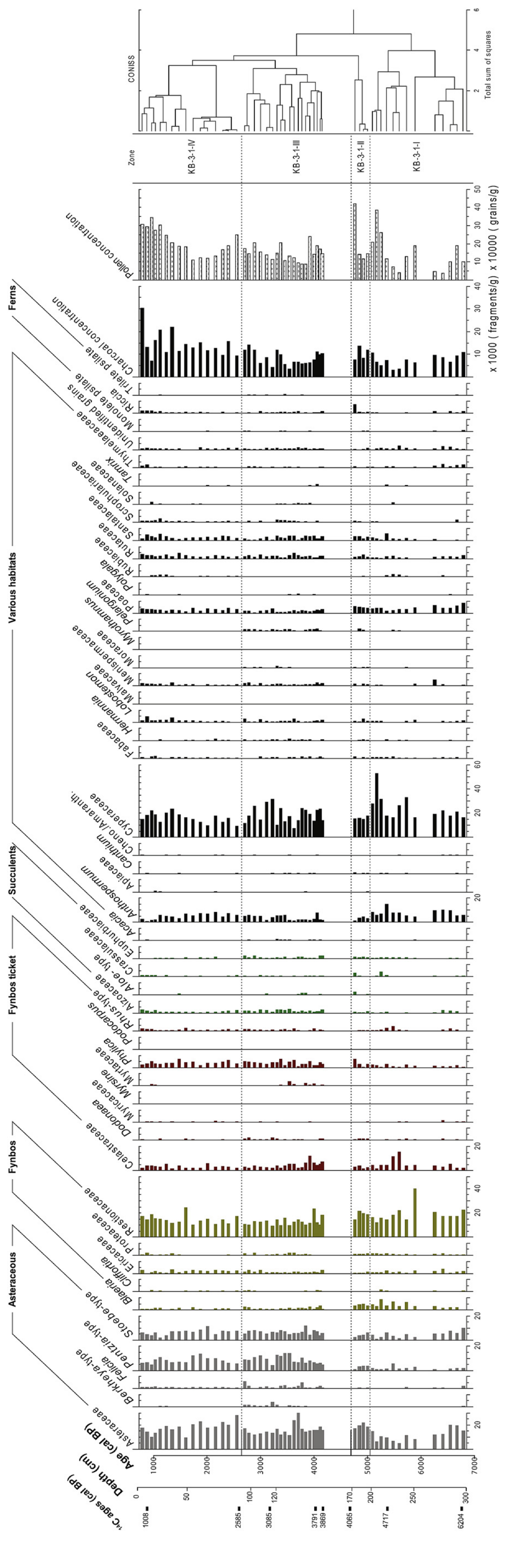

Fig. 4. Pollen percentages and microcharcoal concentration diagram for the KB-3-1 hyrax midden.

with the broad trends in the stable isotope records can be determined according to this framework. Pollen zone KB-3-1-1 is defined by increasing percentages of Celastraceae, Santalaceae, *Blaeria* and Pentzia-type pollen, and decreasing amounts of Aizoaceae, Asteraceae, Poaceae, and *Stoebe*-type pollen and microcharcoal. These trends peak late in KB-3-1-1, at ~5500 cal BP, before, with the exception of Santalaceae, reversing in zone KB-3-1-2. Both *Rhus*-type and *Anthospermum*-type pollen also peak around 5500 cal BP before also declining in KB-3-1-2. Zone KB-3-1-2 is marked by the increase of Asteraceae and the more regular presence of Santalaceae and Rutaceae. The beginning of zone KB-3-1-3, at ~4200 cal BP, is marked by the more regular presence of Aizoaceae, Euphorbiacae, Scrophulariaceae and *Pelargonium*, increases in *Pentzia*-type and *Stoebe*-type pollen, and also elevated percentages of pollen from fynbos thicket taxa such as Celastraceae, Myrtaceae, *Phylica*, and *Rhus*-type. A decline in fynbos thicket taxa is observed at ~3200 cal BP, and is coupled to some degree with an increase in microcharcoal concentrations. After ~2700 cal BP, Aizoaceae, Euphorbiacae and *Pelargonium* decline, along with *Lobostemon*, *Felicia*, and *Dodonaea*, and remain at low levels until the end of zone KB-3-1-3, at ~1300 cal BP. Zone KB-3-1-4 sees a slight increase in Santalaceae, Rubiaceae and Aizoaceae, and high concentrations of microcharcoal.

3.4. pdf-based climate reconstructions

Whereas pollen counts from KB-3-1 indicate only muted environmental/vegetation change, the analysis of these data using the CREST software package (Chevalier et al., 2014) reveals coherent patterns of seasonal precipitation change. To quantify the sensitivity of each reconstructed value to each pollen-type we have used the leave-one-out cross-validation method (LOOCV) proposed in CREST. This provides a direct measurement of the relative importance of each pollen-type, calculating the difference between the reconstruction without the pollen-type of interest (left out) and the reconstruction with all the pollen types (Fig. 5). Broadly speaking, Santalaceae, Celastraceae and Rubiaceae indicate wetter summers at Katbakkies while Aizoaceae, *Lobostemon* or *Felicia* indicate dry summers (Fig. 5). During the course of the record, summer precipitation varies between 30 and 90 mm (Fig. 6). An initial strong increase (+50 mm) is observed from ~6900 to 5500 cal BP, followed by slight (20 mm) progressive decrease until 4900 cal BP. A subsequent period of relative stability is observed until 3300 cal BP, with the exception a severe drought event at 3700–3800 cal BP. Low summer rain is reconstructed for the period from 3200 to 2700 cal BP, followed by a peak (90 mm) between 2500 and 2600 cal BP. Late Holocene summer precipitation stabilises around 60 mm. This is higher than modern summer (DJF) mean precipitation values (~30 mm; Hijmans et al., 2005), but the lower resolution pollen record may not be adequately characterizing the rapid aridification that is observed for this period in the stable isotope record.

Reconstructions of summer and winter rain are in antiphase throughout most of the sequence (Fig. 6). Winter rain decreases from the beginning of the record until ~5500 cal BP. A return to mid-Holocene conditions is reconstructed at ~5200 cal BP. The transition to the late Holocene is associated with drier winter conditions, conditions that prevail until ~1700 cal BP. The last 1000 years of the sequence seems to be associated with a return to wetter winters. The LOOCV (Fig. 5) indicates that winter wet conditions are associated with *Lobostemon*, Solanaceae, Proteaceae and *Leucadendron*.

The difference between summer and winter rain reflects the seasonality of precipitation. Winter rainfall is higher than summer rain in almost all the reconstructed samples except for five samples

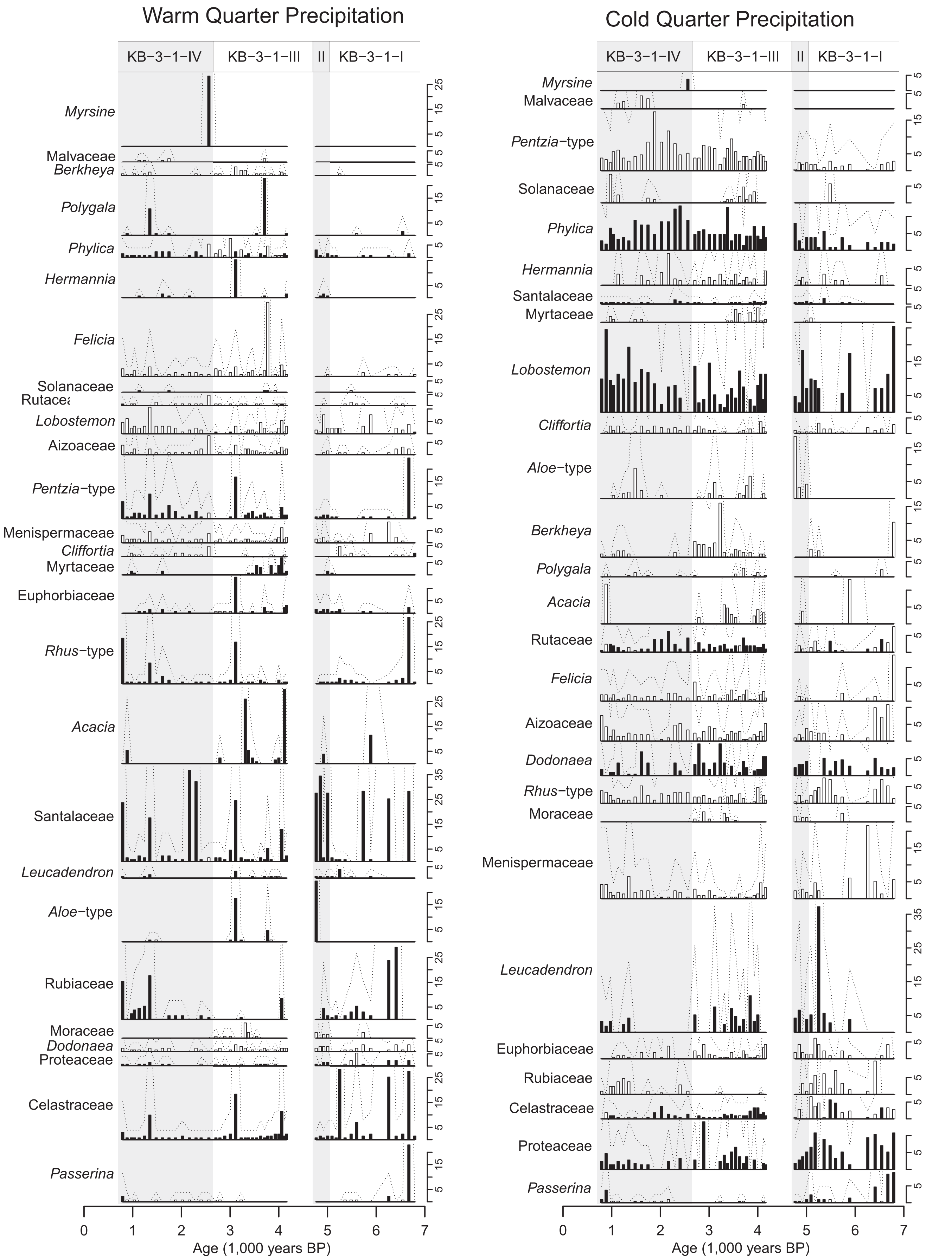

Fig. 5. Results of the leave-one-out cross-validation (LOOCV) analysis of the KB-3-1 pollen sequence. The importance of the pollen types for the reconstruction of the warm (right) and cold (left) quarter precipitation is indicated by the length of the bars, as is their influence in terms of reconstructing wetter (black bars) or drier conditions (white bars) for a given sample.

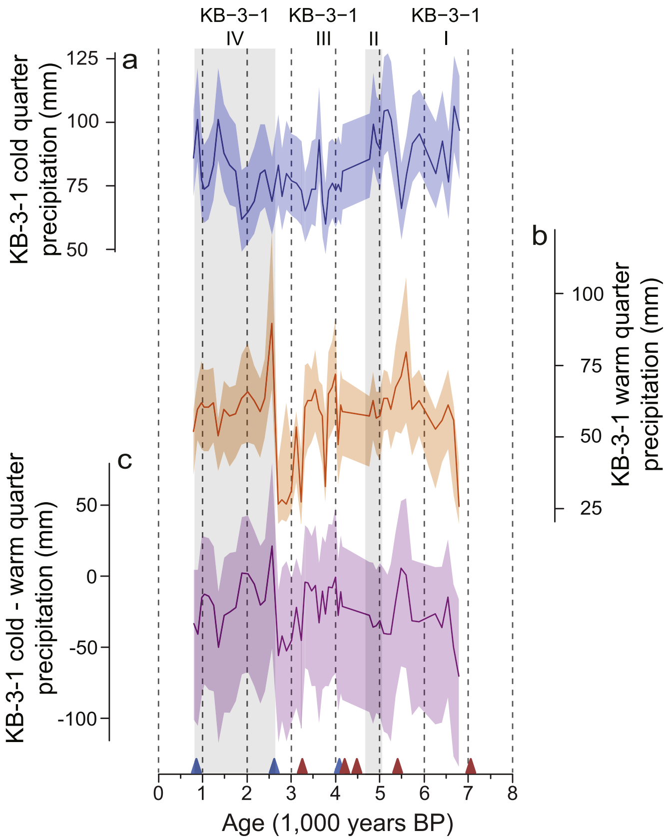

Fig. 6. Reconstruction with 20% errors of cold (a) and warm (b) quarter (winter and summer) precipitation, and the difference between the two as an indicator of seasonality intensity (c) at KB-3-1 derived from the pollen data using the CREST software package (Chevalier et al., 2014).

corresponding to the wettest periods observed at 5600–5500, 2600 and 1900–2000 cal BP, matching wet periods identified with the isotopes. The correlation between the stable isotope records and the difference between the summer and winter precipitation is highly significant ($r^2 = 0.59$, $p < 10^{-4}$), even with small differences in the age–depth models.

4. Discussion

Considered in their regional context, the records obtained from KB-3-1 stand out by virtue of their high resolution, and their clear coherence with other data that allows for robust conclusions to be drawn regarding their palaeoclimatic significance. Considering the strong links identified between humidity, cool conditions and enhanced westerly influence at the Seweweekspoort hyrax midden site (SWP-1 in Fig. 1; Chase et al., 2013), the results from KB-3-1, which is closer to the core of the winter rainfall zone, are perhaps unexpected. As discussed by Chase et al. (2013), enriched $\delta^{15}N$ values (drier conditions) at Seweweekspoort (SWP-1, particularly 7000–5500 cal BP and 4500–3500 cal BP) coincide with elevated continental temperatures, as reconstructed from the Cango Cave $\delta^{18}O$ record (Talma and Vogel, 1992) and lower southern Cape SSTs, which indicate stronger local upwelling with increased easterly flow (Cohen and Tyson, 1995). This mechanistic relationship is further substantiated by records from the Benguela upwelling system along the west coast, which indicate a coeval increase in SSTs, and thus a reduction in upwelling intensity during this period (Farmer et al., 2005; Fig. 7). As intensifications in Benguela upwelling create a high pressure system that limits easterly flow across the continent (Tyson, 1986), these contrasting SST records combine to serve as an integrated indicator of easterly flow in southwestern Africa. At Seweweekspoort, patterns of climate change during the Holocene exhibit an antiphase relationship with easterly flow, highlighting the influence and particular importance of the westerly storm tracks and winter rainfall in the southern Cape during this period.

In contrast, rather than showing a positive relationship between humidity and the inferred proximity of the westerly storm tracks, an anti-phase relationship is observed between the Katbakkies and Seweweekspoort sites (Fig. 7). Allowing for differences in the amplitude of the signals, increases in humidity inferred from the $\delta^{13}C$ and $\delta^{15}N$ records from KB-3-1 are matched by enrichments in the $\delta^{15}N$ record from the SWP-1-5 at millennial to sub-centennial timescales, indicating more arid conditions. As opposed to the Seweweekspoort records, increased humidity at Katbakkies correlates strongly with increased easterly flow, indicating that variations in summer rainfall are of critical importance in determining moisture availability at the site.

These findings are strongly supported by reconstructions based on the pollen data (Fig. 7c, f). While clear trends are not evident in the raw pollen data (Fig. 4), and interpretation of the observed variability is not straightforward, the CREST reconstructions indicate variations in rainfall seasonality that is coherent with both the $\delta^{13}C$ and $\delta^{15}N$ records. Comparisons of the records from Katbakkies demonstrate that increased humidity at the site does not correlate with increased winter rain, but on the contrary it is variability in summer rain that has the strongest impact on changes in humidity at the site. These findings 1) support the hypothesis of Cohen and Tyson (1995) that warmer continental conditions and increased easterly flow would result in more humid conditions in the interior, and 2) highlight that an antiphase relationship existed between temperate and tropical moisture-bearing systems in South Africa during at least the mid-to late Holocene (Tyson, 1986; Cockroft et al., 1988; Tyson et al., 2001).

Combined, the KB-3-1 records indicate significant, coherent patterns of regional climate variability during the mid-to late Holocene. From 6900 to 5600 cal BP, a marked increase in easterly flow (Fig. 7b) resulted in an estimated tripling in summer rainfall (Fig. 7c), and a clear shift to generally more humid conditions (Fig. 7d, e). Winter rainfall generally declined during this period, likely as a result of poleward shifts of the westerly storm track (Lamy et al., 2001) linked with the retreat of Antarctic sea ice (Stuut et al., 2004; Fischer et al., 2007; Divine et al., 2010; Wolff et al., 2010) (Fig. 7f, g, h, i). The period from 5600 to 4700 cal BP sees a reversal of this trend; with a significant expansion of Antarctic sea (Fischer et al., 2007), an equatorward shift of the westerly storm track (Lamy et al., 2001; Chase et al., 2013) and an increase in winter rain at Katbakkies. The coeval reduction of summer rain at Katbakkies during this period resulted in slightly drier conditions at the site. After 4700 cal BP, a southward shift of the westerlies results in increased easterly flow, and wetter conditions with increased summer rainfall at Katbakkies. Apart from a marked aridification event from 3900 to 3800 cal BP, conditions remained relatively humid until 3200 cal BP, when there was an abrupt shift (<30 years) to a period of significantly drier conditions, with intensified rainfall seasonality, that lasted until 2800 cal BP. An equally abrupt increase in summer rainfall at 2700 cal BP, once again reduced rainfall seasonality and led to a relatively humid period that lasted until ~1600 cal BP, after which broad scale cooling is reflected in increased Antarctic sea ice, and northward shift of the westerlies and an increase in winter rainfall in the SW Cape (Fig. 7). At Katbakkies, these changes led to a long-term decline in moisture availability until the end of the record at 700 cal BP.

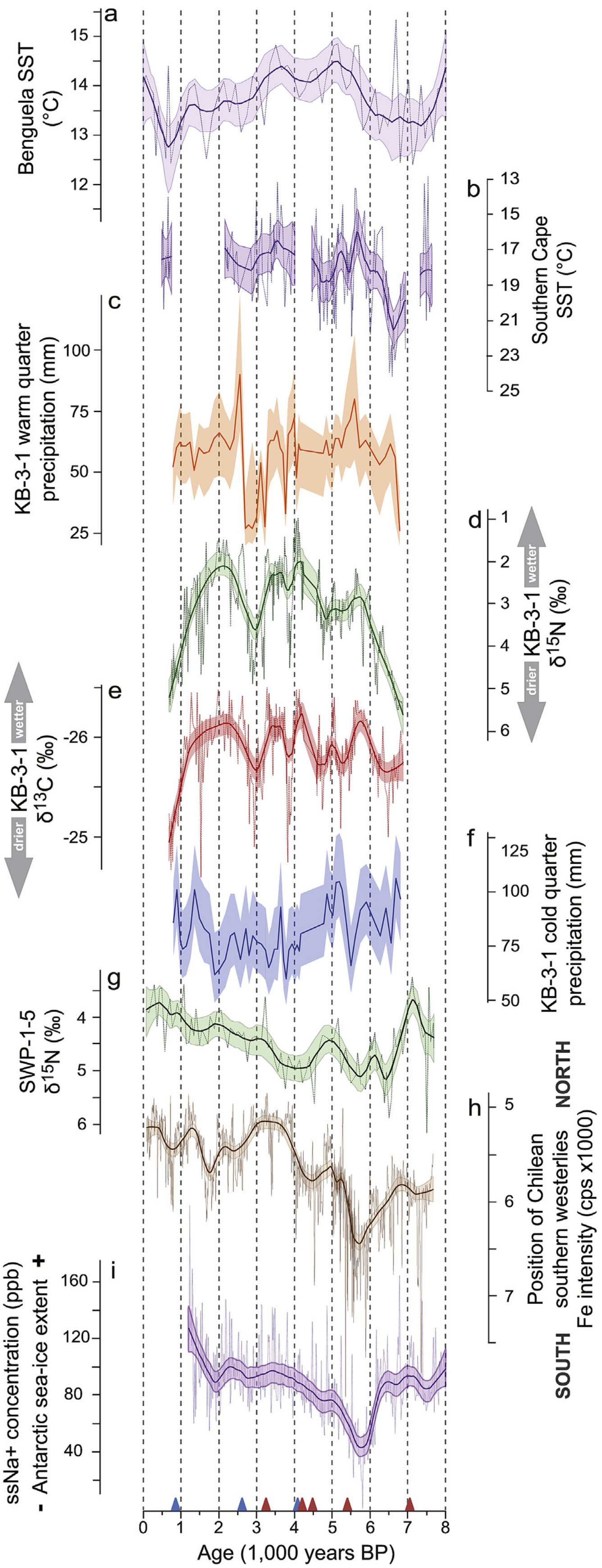

Fig. 7. Comparison of $\delta^{15}N$ (d) and $\delta^{13}C$ values (e) and reconstructions of summer (c) and winter (f) rainfall (20% error shaded) for the KB-3-1 hyrax middens with regional palaeoenvironmental records including sea-surface temperatures from the Benguela (a; Farmer et al., 2005)) and south coast (b; Cohen and Tyson, 1995)) upwelling regions, variations in moisture availability reflected in the Seweweekspoort-1-5 $\delta^{15}N$ record (g; Chase et al., 2013), iron concentrations from the Chilean continental margin at 41°S indicating the latitudinal position of the westerly storm track (h; Lamy et al., 2001) and sea salt sodium concentrations from the EPICA DML ice core in Antarctica reflecting variations in sea ice extent (i; Fischer et al., 2007).

In contextualising these findings into the regional palaeoenvironmental framework, it is important to remember that the discussion of palaeoclimatic trends in the region often centres on rainfall seasonality (Cockroft et al., 1988; Lee-Thorp and Beaumont, 1995; Meadows and Baxter, 1999; Tyson et al., 2001; Partridge et al., 2004; Chase and Meadows, 2007), particularly at locations marginal to the major contemporary rainfall zones. This must be considered, to an extent, as distinct from changes in absolute rainfall, as in many regions it is the length and intensity of the drought season that is the primary climatic determinant of environmental change inferred from ecological proxies. For instance, Katbakkies currently receives ~62% of its precipitation between May and August, with ~40–50 mm falling in each month (Hijmans et al., 2005). From September through March, less than 15 mm of monthly precipitation is received. This is typically poorly distributed throughout each month, and as this period coincides with maximum temperatures and potential evapotranspiration, the regional growing season is therefore sharply restricted to the austral winter. While an equatorward shift of the westerlies may bring more rainfall to Katbakkies during the winter months, and the rainy season may perhaps be extended (Chase and Meadows, 2007), a significant drought period may still persist. In the context of this study therefore, an increase in easterly flow during the austral summer would have a more significant impact on overall water availability, as it would more directly limit the length and intensity of the drought season. The importance of the reduction in drought season length/intensity on humidity at Katbakkies is clearly highlighted when the ratio between winter and summer rain, as derived from the CREST reconstructions, is calculated. Compared with the stable isotope records, it is apparent that much of the variability in humidity can be attributed to this dynamic (Fig. 7).

That evidence for increased humidity in the winter rainfall zone does not necessarily reflect changes in winter rainfall, while being apparently counter-intuitive, is supported by data from nearby sites such as De Rif in the Cederberg Mountains. At De Rif, a strong positive relationship has been observed between water availability and SSTs in the Benguela upwelling region (Chase et al., 2011). While this may be seen to contradict prevailing conceptual models wherein cooler global conditions result in an expansion of the circumpolar vortex and increased humidity in the winter rainfall zone (van Zinderen Bakker, 1976; Cockcroft et al., 1987; Chase and Meadows, 2007), it is consistent with the proposition that increased precipitation during the drought season will have substantially greater impact in limiting annual drought stress, and its reflection in the hyrax midden stable isotope records.

Throughout the KB-3-1 record, a general antiphase relationship is observed between temperate and tropical rainfall, supporting models regarding the nature of the long-term dynamic of these systems (Tyson, 1986, 1991, 1999; Cockcroft et al., 1987; Tyson et al., 2002). The consideration that the increased influence of temperate systems will result in more humid conditions in the winter rainfall zone (Weldeab et al., 2013), however, is significantly refined by the data presented here. While more precipitation during the rainy season would, all other things being equal, result in increased annual precipitation, it did not appear to significantly attenuate drought stress during the period covered by this record. Of greater environmental significance were increases in dry season rainfall, which more effectively reduce drought stress and result in more significant changes in overall moisture availability.

5. Conclusions

- We present new, continuous pollen, microcharcoal and high resolution $\delta^{15}N$ and $\delta^{13}C$ records that reflect Holocene climates in a poorly understood, but particularly dynamic region of southern Africa.
- Previously considered to have experienced relatively little environmental change during the Holocene (Meadows and Sugden, 1991; Meadows et al., 2010), the data presented here indicate significant, abrupt changes, that are linked to similar variability in the region's dominant climate systems.
- While the pollen record exhibits limited variability, analysis with the CREST software package (Chevalier et al., 2014), employing *pdf*-based modelling techniques, has allowed for the extraction of coherent records of variations in rainfall seasonality.
- The comparison of the $\delta^{15}N$ and $\delta^{13}C$ records (that primarily reflect water-availability in the environment) with the reconstructions of rainfall seasonality indicates that while the site is located in the winter rainfall zone, it is summer rainfall variability that has the greatest impact on water-availability at the site.
- Variations in summer rainfall are linked to upwelling intensity in the Benguela system (Farmer et al., 2005) and along the south coast; wherein reduced Benguela upwelling allows for increased easterly flow and upwelling along the south coast (Cohen and Tyson, 1995), and the more effective propagation of easterly waves; bringing increased rainfall to the interior during the summer months (Tyson, 1986; Cohen and Tyson, 1995).
- Coeval inverse trends revealed in the records from Katbakkies and nearby Seweweekspoort are consistent with the mechanisms determining the dynamics and relative influence of the primary opposing tropical and temperate climate systems in South Africa. Combined they provide a coherent picture of Holocene climate change in the region, and link regional variability with changes in global boundary conditions.

Acknowledgements

Funding was received from the European Research Council (ERC) under the European Union's Seventh Framework Programme (FP7/2007–2013)/ERC Starting Grant “HYRAX”, grant agreement no. 258657. The South African National Biodiversity Institute is thanked for the use of data/information supplied by SANBI from digitized collections. We would like to thank Tracey Nowell and Ian Newton for assistance in collecting and analysing the material.

Appendix A. Supplementary data

Supplementary data related to this article can be found at http://dx.doi.org/10.1016/j.quascirev.2014.10.011.

References

Blaauw, M., Christen, J.A., 2011. Flexible Paleoclimate age-depth models using an Autoregressive Gamma Process. Bayesian Anal. 6, 457–474.
Boom, A., Carr, A.S., Chase, B.M., Grimes, H.L., Meadows, M.E., 2014. Leaf wax n-alkanes and $\delta^{13}C$ values of CAM plants from arid southwest Africa. Org. Geochem. 67, 99–102.
Carr, A.S., Thomas, D.S.G., Bateman, M.D., Meadows, M.E., Chase, B., 2006. Late Quaternary palaeoenvironments of the winter-rainfall zone of southern Africa: palynological and sedimentological evidence from the Agulhas Plain. Palaeogeogr. Palaeoclimatol. Palaeoecol. 239, 147–165.
Chase, B.M., Boom, A., Carr, A.S., Meadows, M.E., Reimer, P.J., 2013. Holocene climate change in southernmost South Africa: rock hyrax middens record shifts in the southern westerlies. Quat. Sci. Rev. 82, 199–205.
Chase, B.M., Meadows, M.E., 2007. Late Quaternary dynamics of southern Africa's winter rainfall zone. Earth-Sci. Rev. 84, 103–138.
Chase, B.M., Meadows, M.E., Carr, A.S., Reimer, P.J., 2010. Evidence for progressive Holocene aridification in southern Africa recorded in Namibian hyrax middens: implications for African Monsoon dynamics and the “African Humid Period”. Quat. Res. 74, 36–45.
Chase, B.M., Meadows, M.E., Scott, L., Thomas, D.S.G., Marais, E., Sealy, J., Reimer, P.J., 2009. A record of rapid Holocene climate change preserved in hyrax middens from southwestern Africa. Geology 37, 703–706.
Chase, B.M., Quick, L.J., Meadows, M.E., Scott, L., Thomas, D.S.G., Reimer, P.J., 2011. Late glacial interhemispheric climate dynamics revealed in South African hyrax middens. Geology 39, 19–22.
Chase, B.M., Scott, L., Meadows, M.E., Gil-Romera, G., Boom, A., Carr, A.S., Reimer, P.J., Truc, L., Valsecchi, V., Quick, L.J., 2012. Rock hyrax middens: a palaeoenvironmental archive for southern African drylands. Quat. Sci. Rev. 56, 107–125.
Chevalier, L., Cheddadi, R., Chase, B.M., 2014. CREST: a pdf-based quantitative climate reconstruction method. Clim. Past (in press).
Clark, J.S., 1988. Stratigraphic charcoal analysis on petrographic thin section: application to fire history in northwestern Minnesota. Quat. Res. 30, 81–91.
Cockcroft, M.J., Wilkinson, M.J., Tyson, P.D., 1987. The application of a present-day climatic model to the late Quaternary in southern Africa. Clim. Change 10, 161–181.
Cockroft, M.J., Wilkinson, M.J., Tyson, P.D., 1988. A palaeoclimatic model for the late Quaternary in southern Africa. Palaeoecol. Afr. 19, 279–282.
Cohen, A.L., Parkington, J.E., Brundrit, G.B., van der Merwe, N.J., 1992. A Holocene marine climate record in mollusc shells from the Southwest African coast. Quat. Res. 38, 379–385.
Cohen, A.L., Tyson, P.D., 1995. Sea surface temperature fluctuations during the Holocene off the south coast of Africa: implications for terrestrial climate and rainfall. Holocene 5, 304–312.
Conedera, M., Tinner, W., Neff, C., Meurer, M., Dickens, A.F., Krebs, P., 2009. Reconstructing past fire regimes: methods, applications, and relevance to fire management and conservation. Quat. Sci. Rev. 28, 555–576.
Craine, J.M., Elmore, A.J., Aidar, M.P.M., Bustamante, M., Dawson, T.E., Hobbie, E.A., Kahmen, A., Mack, M.C., McLauchlan, K.K., Michelsen, A., Nardoto, G.B., Pardo, L.H., Peñuelas, J., Reich, P.B., Schuur, E.A.G., Stock, W.D., Templer, P.H., Virginia, R.A., Welker, J.M., Wright, I.J., 2009. Global patterns of foliar nitrogen isotopes and their relationships with climate, mycorrhizal fungi, foliar nutrient concentrations, and nitrogen availability. New Phytol. 183, 980–992.
Divine, D.V., Koç, N., Isaksson, E., Nielsen, S., Crosta, X., Godtliebsen, F., 2010. Holocene Antarctic climate variability from ice and marine sediment cores: insights on ocean–atmosphere interaction. Quat. Sci. Rev. 29, 303–312.
Ehleringer, J.R., Cooper, T.A., 1988. Correlations between carbon isotope ratio and microhabitat of desert plants. Oecologia 76, 562–566.
Farmer, E.C., deMenocal, P.B., Marchitto, T.M., 2005. Holocene and deglacial ocean temperature variability in the Benguela upwelling region: implications for low-latitude atmospheric circulation. Paleoceanography 20. http://dx.doi.org/10.1029/2004PA001049.
Fischer, H., Fundel, F., Ruth, U., Twarloh, B., Wegner, A., Udisti, R., Becagli, S., Castellano, E., Morganti, A., Severi, M., Wolff, E., Littot, G., Röthlisberger, R., Mulvaney, R., Hutterli, M.A., Kaufmann, P., Federer, U., Lambert, F., Bigler, M., Hansson, M., Jonsell, U., de Angelis, M., Boutron, C., Siggaard-Andersen, M.-L., Steffensen, J.P., Barbante, C., Gaspari, V., Gabrielli, P., Wagenbach, D., 2007. Reconstruction of millennial changes in dust emission, transport and regional sea ice coverage using the deep EPICA ice cores from the Atlantic and Indian Ocean sector of Antarctica. Earth Planet. Sci. Lett. 260, 340–354.
Grimm, E.C., 2011. Tilia Version 1.7.16.
Hartman, G., 2011. Are elevated $\delta^{15}N$ values in herbivores in hot and arid environments caused by diet or animal physiology? Funct. Ecol. 25, 122–131.
Hartman, G., Danin, A., 2010. Isotopic values of plants in relation to water availability in the Eastern Mediterranean region. Oecologia 162, 837–852.
Hijmans, R., Cameron, S.E., Parra, J.L., Jones, P.G., Jarvis, A., 2005. Very high resolution interpolated climate surfaces for global land areas. Int. J. Climatol. 25, 1965–1978.
Hogg, A.G., Hua, Q., Blackwell, P.G., Niu, M., Buck, C.E., Guilderson, T.P., Heaton, T.J., Palmer, J.G., Reimer, P.J., Reimer, R.W., Turney, C.S.M., Zimmerman, S.R.H., 2013. SHCal13 Southern Hemisphere Calibration, 0–50,000 Years cal BP.
Lamy, F., Hebbeln, D., Rohl, U., Wefer, G., 2001. Holocene rainfall variability in southern Chile: a marine record of latitudinal shifts of the Southern Westerlies. Earth Planet. Sci. Lett. 185, 369–382.
Lee-Thorp, J.A., Beaumont, P.B., 1995. Vegetation and seasonality shifts during the late Quaternary deduced from $^{13}C/^{12}C$ ratios of grazers at Equus Cave, South Africa. Quat. Res. 43, 426–432.
Martin, A.R.H., 1968. Pollen analysis of Groenvlei lake sediments, Knysna (South Africa). Rev. Palaeobot. Palynol. 7, 107–144.
Meadows, M.E., Baxter, A.J., 1999. Late Quaternary palaeoenvironments of the southwestern Cape, South Africa: a regional synthesis. Quat. Int. 57–58, 193–206.
Meadows, M.E., Chase, B.M., Seliane, M., 2010. Holocene palaeoenvironments of the Cederberg and Swartruggens mountains, Western Cape, South Africa: pollen and stable isotope evidence from hyrax dung middens. J. Arid Environ. 74, 786–793.

Meadows, M.E., Sugden, J.M., 1991. A vegetation history of the last 14,000 years on the Cederberg, southwestern Cape Province. South Afr. J. Sci. 87, 34–43.

Meadows, M.E., Sugden, J.M., 1993. The late Quaternary palaeoecology of a floristic kingdom: the southwestern Cape, South Africa. Palaeogeogr. Palaeoclimatol. Palaeoecol. 101, 271–281.

Moore, P.D., Webb, J.A., Collinson, M.E., 1991. Pollen Analysis. Blackwell Scientific Publications, London.

Mucina, L., Rutherford, M.C., 2006. The Vegetation of South Africa, Lesotho and Swaziland, Strelitzia. South African National Biodiversity Institute, Pretoria.

Murphy, B.P., Bowman, D.M.J.S., 2006. Kangaroo metabolism does not cause the relationship between bone collagen $\delta^{15}N$ and water availability. Funct. Ecol. 20, 1062–1069.

Newsome, S.D., Miller, G.H., Magee, J.W., Fogel, M.L., 2011. Quaternary record of aridity and mean annual precipitation based on $\delta^{15}N$ in ratite and dromornithid eggshells from Lake Eyre, Australia. Oecologia 167, 1151–1162.

Partridge, T.C., Scott, L., Schneider, R.R., 2004. Between Agulhas and Benguela: responses of southern African climates of the late Pleistocene to current fluxes, orbital precession and the extent of the circum-Antarctic vortex. Past Clim. Var. Eur. Afr. 45–68.

Pate, J.S., 2001. Carbon isotope discrimination and plant water-use efficiency: case scenarios for C_3 plants. In: Unkovich, M., Pate, J., McNeill, A., Gibbs, D.J. (Eds.), Stable Isotope Techniques in the Study of Biological Processes and Functioning of Ecosystems. Kluwer Academic Publishers, Dordrecht, pp. 19–37.

Peri, P.L., Ladd, B., Pepper, D.A., Bonser, S.P., Laffan, S.W., Amelung, W., 2012. Carbon ($\delta^{13}C$) and nitrogen ($\delta^{15}N$) stable isotope composition in plant and soil in Southern Patagonia's native forests. Glob. Change Biol. 18, 311–321.

Quick, L.J., Chase, B.M., Meadows, M.E., Scott, L., Reimer, P.J., 2011. A 19.5 kyr vegetation history from the central Cederberg Mountains, South Africa: palynological evidence from rock hyrax middens. Palaeogeogr. Palaeoclimatol. Palaeoecol. 309, 253–270.

Rutherford, M.C., Mucina, L., Powrie, L.W., 2012. The South African national vegetation database: history, development, applications, problems and future. S. Afr. J. Sci. 108.

Rutherford, M.C., Powrie, L.W., Midgley, G.F., 2013. ACKDAT: a digital spatial database of distributions of South African plant species and species assemblages. S. Afr. J. Bot. 69, 99–104.

SANBI, 2003. PRECIS (National Herbarium Pretoria (PRE) Computerized Information System) database.

Scholtz, A., 1986. Palynological and Palaeobotanical Studies in the Southern Cape. University of Stellenbosch, Stellenbosch, South Africa.

Scott, L., 1982. Late Quaternary fossil pollen grains from the Transvaal, South Africa. Rev. Palaeobot. Palynol. 36, 241–278.

Scott, L., Woodborne, S., 2007a. Pollen analysis and dating of Late Quaternary faecal deposits (hyraceum) in the Cederberg, Western Cape, South Africa. Rev. Palaeobot. Palynol. 144, 123–134.

Scott, L., Woodborne, S., 2007b. Vegetation history inferred from pollen in Late Quaternary faecal deposits (hyraceum) in the Cape winter-rain region and its bearing on past climates in South Africa. Quat. Sci. Rev. 26, 941–953.

Stockmarr, J., 1971. Tablets with spores used in absolute pollen analysis. Pollen Spores 13, 614–621.

Stuut, J.-B.W., Crosta, X., Van der Borg, K., Schneider, R.R., 2004. On the relationship between Antarctic sea ice and southwestern African climate during the late Quaternary. Geology 32, 909–912.

Talma, A.S., Vogel, J.C., 1992. Late Quaternary paleotemperatures derived from a speleothem from Cango Caves, Cape Province, South Africa. Quat. Res. 37, 203–213.

Tinner, W., Conedera, M., Ammann, B., Gaeggler, H.W., Gedye, S., Jones, R., Saegesser, B., 1998. Pollen and charcoal in lake sediments compared with historically documented forest fires in southern Switzerland since AD 1920. Holocene 8, 31–42.

Tyson, P.D., 1986. Climatic Change and Variability in Southern Africa. Oxford University Press, Cape Town.

Tyson, P.D., 1991. Climatic change in southern Africa: past and present conditions and possible future scenarios. Clim. Change 18, 241–258.

Tyson, P.D., 1999. Atmospheric circulation changes and palaeoclimates of southern Africa. South Afr. J. Sci. 95, 194–201.

Tyson, P.D., Cooper, G.R.J., McCarthy, T.S., 2002. Millennial to multi-decadal variability in the climate of southern Africa. Int. J. Climatol. 22, 1105–1117.

Tyson, P.D., Odada, E.O., Partridge, T.C., 2001. Late Quaternary environmental change in southern Africa. South Afr. J. Sci. 97, 139–150.

Tyson, P.D., Preston-Whyte, R.A., 2000. The Weather and Climate of Southern Africa. Oxford University Press, Cape Town.

Valsecchi, V., Chase, B.M., Slingsby, J.A., Carr, A.S., Quick, L.J., Meadows, M.E., Cheddadi, R., Reimer, P.J., 2013. A high resolution 15,600-year pollen and microcharcoal record from the Cederberg Mountains, South Africa. Palaeogeogr. Palaeoclimatol. Palaeoecol. 387, 6–16.

van Zinderen Bakker, E.M., 1953. South African Pollen Grains and Spores. Part I. Balkema, Amsterdam/Cape Town.

van Zinderen Bakker, E.M., 1956. South African Pollen Grains and Spores. Part II. Balkema, Amsterdam/Cape Town.

van Zinderen Bakker, E.M., 1976. The evolution of late Quaternary paleoclimates of Southern Africa. Palaeoecol. Afr. 9, 160–202.

van Zinderen Bakker, E.M., Coetzee, J.A., 1959. South African Pollen Grains and Spores. Part III. Balkema, Amsterdam/Cape Town.

Weldeab, S., Stuut, J.B.W., Schneider, R.R., Siebel, W., 2013. Holocene climate variability in the winter rainfall zone of South Africa. Clim. Past. 9, 2347–2364.

Wolff, E.W., Barbante, C., Becagli, S., Bigler, M., Boutron, C.F., Castellano, E., de Angelis, M., Federer, U., Fischer, H., Fundel, F., Hansson, M., Hutterli, M., Jonsell, U., Karlin, T., Kaufmann, P., Lambert, F., Littot, G.C., Mulvaney, R., Röthlisberger, R., Ruth, U., Severi, M., Siggaard-Andersen, M.L., Sime, L.C., Steffensen, J.P., Stocker, T.F., Traversi, R., Twarloh, B., Udisti, R., Wagenbach, D., Wegner, A., 2010. Changes in environment over the last 800,000 years from chemical analysis of the EPICA Dome C ice core. Quat. Sci. Rev. 29, 285–295.